Polymer 42 (2001) 7395–7401

polymer

www.elsevier.nl/locate/polymer

Rheological behaviour of solutions of poly(2-hydroxyethyl methacrylamide) in glycerine

Serguei R. Kosvintsev[a,b], Evaristo Riande[b,*], Manuel G. Velarde[c], Julio Guzmán[b]

[a]*Department of Chemical Engineering, Loughborough University, Loughborough, Leicestershire, UK*
[b]*Instituto de Ciencia y Tecnología de Polímeros (CSIC), 28006 Madrid, Spain*
[c]*Instituto Pluridisciplinar, Universidad Complutense, 28008 Madrid, Spain*

Received 4 September 2000; received in revised form 19 January 2001; accepted 8 March 2001

Abstract

The rheological behaviour of dilute and semidilute solutions of poly(2-hydroxyethyl methacrylamide) in glycerine is described, emphasising the study of the variation of both the zero shear rate viscosity, η_0, and the steady-state compliance function, J_e^0, with concentration. Shear rate fields, above a critical value, may promote molecular tight 'structures' that enhance the viscosity of the semidilute solutions and, as a result, these systems exhibit shear-thickening behaviour. However, the dilute solutions display shear-thinning behaviour and obey the Cox–Merz rule. The flow transients appearing after either application of a constant shear rate or cessation of flow were studied for semidilute solutions. The shear-thickening behaviour of these solutions is interpreted in terms of the formation of hydrogen bonds between the acrylamide groups and the carbonyl groups of different chains. © 2001 Elsevier Science Ltd. All rights reserved.

Keywords: Polymer solutions; Shear thickening; Shear thinning

1. Introduction

The viscoelasticity of polymer melts and solutions plays an important role in the transient and complex flows encountered in a variety of flow processes. The flow behaviour of polymer melts depends on the chain size, molecular weight distribution, chain flexibility, and shear rate. The rheology of polymer solutions also depends on concentration, and polymer–solvent interactions may play an important role in the flow behaviour of both dilute and very dilute solutions.

In general, the phenomenological theory of viscoelasticity suggests some correlations between the functions that characterise the steady-state condition of a shearing flow, and the functions describing the dynamic properties of the system in the linear viscoelastic regime [1–5]. Specifically, the viscosity obtained from a simple shear flow process ($\eta = \sigma/\dot{\gamma}$, where σ and $\dot{\gamma}$ are, respectively, the shear stress and the shear rate) is compared with the dynamic viscosity η' ($= G''(\omega)/\omega$, where G'' (ω) is the loss relaxation modulus at the frequency ω) [1], whereas the first normal stress difference coefficient $N_1\{ = (\sigma_{11} - \sigma_{22})/2\dot{\gamma}^2\}$ is related to the coefficient $A_G = G'(\omega)/\omega^2$. On the other hand, $N_1(\dot{\gamma})$ and $G'(\omega)$ are related with the elasticity of the material, i.e. its ability to store the work of external forces.

Both the storage and loss relaxation moduli show a rather complicated dependence on frequency dictated by the salient features of the relaxation spectrum of the system and, in principle, no correlation between $\eta'(\omega)$ and $\eta(\dot{\gamma})$ should be expected to exist with the exception of the limiting point

$$\eta_0 = \lim_{\omega \to 0} \eta'(\omega) = \lim_{\omega \to 0} \frac{G''(\omega)}{\omega} = \int_0^\infty \tau H(\tau)\mathrm{d}\tau, \qquad (1)$$

where τ and $H(\tau)$ are, respectively, the relaxation time and the relaxation spectrum. However, if we consider that the external effect alters the relaxation spectrum of the system during flow, Eq. (1) can be generalised to describe the dependence of the viscosity on the shear rate by means of the following expression [6]:

$$\eta(\dot{\gamma}) = \int_0^\infty \tau H(\tau, \dot{\gamma})\mathrm{d}\tau, \qquad (2)$$

where $H(\tau, \dot{\gamma})$ is the altered relaxation spectrum that returns to the spectrum corresponding to the undeformed state at $\dot{\gamma} \to 0$. Based on this reasoning, several relationships between $\sigma(\dot{\gamma})$ (or $\sigma_{11} - \sigma_{22}$) and $G''(\omega)$ (or $G'(\omega)$) have been established [7]. Among these, of great interest is the

---

[*] Corresponding author.

PII: S0032-3861(01)00195-1

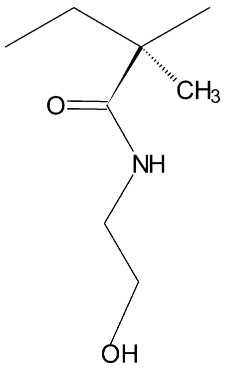

Fig. 1. Structural unit of poly(2-hydroxyethyl methacrylamide).

Cox–Merz [8] empirical method

$$\eta(\dot{\gamma}) = |\eta^*|(\omega) \qquad \text{at } \dot{\gamma} \rightarrow \omega, \tag{3}$$

where $|\eta^*(\omega)| = (1/\omega(G'^2 + G''^2)^{1/2}$ is the absolute value of the complex viscosity.

The kinetic aspects of the polymerisation of methacrylate polymers of hydrophilic character have recently been studied in our laboratories, specifically, poly(2-hydroxyethyl methacrylamide) (PHMCA), and the suitability of this material for the preparation of soft contact lenses is currently being tested. A schematic representation of the repeating unit of this polymer is shown in Fig. 1. In this work, we have studied the rheological behaviour of dilute and semidilute solutions of PHMCA in glycerine, a solvent of low volatility. Thus, the variations of both the zero shear rate viscosity and the steady-state compliance function with the concentration of the solutions were determined. The non-Newtonian character of these solutions was studied using steady flow experiments, and the results compared with those predicted by the Cox–Merz relationship.

2. Experimental part

2.1. Synthesis and characterisation of poly(2-hydroxyethyl methacrylamide)

The monomer, 2-hydroxyethyl methacrylamide, was prepared by adding dropwise a solution of methacyloyl chloride in ethyl ether to 2-aminoethanol dissolved in an aqueous sodium hydroxide solution. The reaction was carried out at 0°C under nitrogen atmosphere. The monomer was purified by means of several extractions with dichloromethane, obtaining a product with purity higher than 99%, as determined by high performance liquid chromatography (HPLC) and gas chromatography.

Poly(2-hydroxyethyl methacrylamide) was obtained by radical polymerisation of 2-hydroxyethyl methacrylamide in a mixture of water–dioxane (50/50), at 60°C, using AIBN as initiator. The reaction was carried out in vacuum, and stopped when a conversion of about 10% was reached. The polymer was isolated from the reaction medium by several precipitations in *n*-hexane and, finally, purified by freeze drying from dioxane–water. The number-average molecular weight of the polymer was 50,000, the dispersion index was roughly 2, and its glass transition temperature, 120°C.

2.1.1. Preparation of polymer–glycerine solutions

A relatively dilute aqueous solution (I) of poly(2-hydroxyethyl methacrylamide) was prepared by dispersing the polymer in water at 60°C under slow mixing conditions. The amount of glycerine required to prepare a solution of about 20% of the polymer in this solvent was added to solution I. Then, the water was removed from the polymer/water–glycerine solution by evaporation at reduced pressure. The concentration of polymer in glycerine was adjusted to the concentrations of interest by adding the required amount of solvent to the primitive solution. The solution was further homogenised under slow stirring conditions.

2.1.2. Steady flow and oscillatory measurements

Both the oscillatory and steady flow of five solutions of weight fractions 0.027, 0.0533, 0.0818, 0.135 and 0.174 were measured. The measurements were carried out with an R-19 Weissenberg rheogoniometer, at room temperature, using cone–plate geometry. For the solutions of lower viscosity ($\eta_0 < 1$ Ns m^{-2}), a cone of 2°, and a plate 50 mm of diameter were used, whereas the angle and the radius were 1° and 25 mm, respectively, for the measurements carried out on the solutions of higher viscosity ($\eta_0 > 10$ Ns m^{-2}). In the oscillatory measurements, the driving amplitude was less than 1.0×10^{-3}, thus ensuring linear regime in the experiments.

Angular displacements were measured with two NA1/2.5 mm linear variable differential transducers (LVDT) connected to a C56R transducer meter, both from Sangamo. The unfiltered output voltages from the transducers were analysed and stored with a four-channel Nicolett System 420 digital oscilloscope. This instrument digitalises the input signals from the cone and plate by means of 12-bit A/D converters. The angular resolution was $\pm 5 \times 10^{-6}$ rad.

In the oscillatory measurements, the digital signals were stored and later processed. The curves obtained were fitted to the functions

$$X_1 = X_{01} \sin(2\pi\omega t + \phi_{01}) + A_1,$$

$$X_2 = X_{01} \sin(2\pi\omega t + \phi_{02}) + A_2, \tag{4}$$

where X_{01}, X_{02}, ϕ_{01}, ϕ_{02}, A_1 and A_2 represent, respectively, amplitudes (X), phase angles (ϕ) and permanent shifts (A) (of the steady component of the signal) of the cone and plate signals, respectively. The ratio of amplitudes b ($= X_{01}/X_{02}$) was determined with an error lower than 3%. However, the error for the phase lag $\Delta\phi$ ($= \phi_{01} - \phi_{02}$) was 5–15% for values of this parameter lying in the vicinity of those corresponding to the difference between the driving frequency and the natural frequency of the instrument. The natural frequencies for the first and second configurations were 75 ± 13 and 340 ± 1 rad s^{-1}, respectively.

3. Results and discussion

3.1. Flow behaviour from dynamic experiments

The rheological behaviour of the solutions was studied in the low frequency region, or terminal region, where flow dominates. The real ($G'(\omega)$) and loss ($G''(\omega)$) components of the complex relaxation modulus ($G^*(\omega)$) of the solutions are plotted, in the frequency domain, in Figs. 2 and 3, respectively. The curves are similar to those displayed by rheological simple systems. Thus, the double logarithmic plots $G'(\omega)$ against ω are straight lines of slope 2 in the limit $\omega \rightarrow 0$, in agreement with the prediction of the phenomenological theory of linear viscoelasticity. Similar plots for $G''(\omega)$ also agree with the predictions of the theory since in the limit $\omega \rightarrow 0$, the curves are straight lines of slope 1. As expected, the curves are shifted to lower frequencies as the concentration increases.

Values of the viscosity at zero shear rate obtained by means of Eq. (1) from Fig. 2 are shown in the third column of Table 1. It can be seen that for dilute solutions, the viscosity only increases moderately with concentration, presumably as a consequence of the fact that the polymer chains in the solutions are slightly entangled. The rather sharp increase in viscosity with concentration for semidilute solutions is apparently a consequence of the increase in the density of entanglements in the solutions.

An important viscoelastic function that accounts for the maximum recoverable deformation is the steady-state compliance, J_e^0. According to the phenomenological theory of linear viscoelasticity [9],

$$J_e^0 = \frac{1}{\eta_0^2} \lim_{\omega \rightarrow 0} \frac{G'(\omega)}{\omega^2} = \frac{\langle \tau \rangle}{\eta_0}, \tag{5}$$

where $\langle \tau \rangle$ is the mean-relaxation time of the solutions. Values of the steady-state compliance of these systems are shown in the third and fourth columns of Table 1. It can be seen that the values of J_e^0 are rather insensitive to the concentration of polymer in the range of concentrations studied.

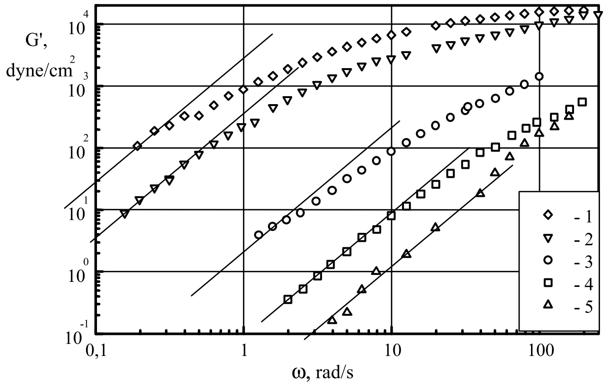

Fig. 2. Frequency dependence of the storage relaxation modulus, at 25° C, for different concentrations: (1) $w = 0.174$, (2) $w = 0.135$, (3) $w = 0.0818$, (4) $w = 0.0533$ and (5) $w = 0.0227$.

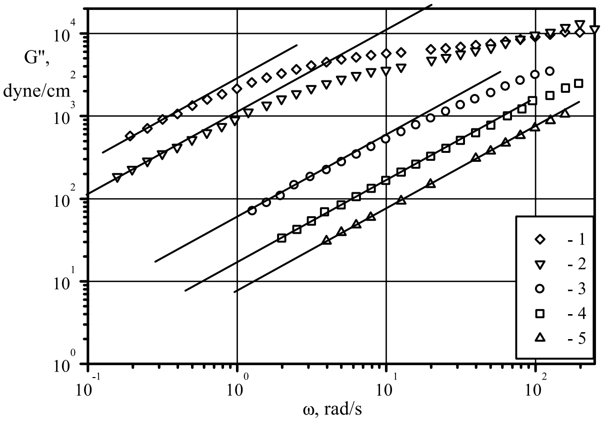

Fig. 3. Variation of the loss relaxation modulus with the angular frequency, at 25° C, for different concentrations: (1) $w = 0.174$, (2) $w = 0.135$, (3) $w = 0.0818$, (4) $w = 0.0533$ and (5) $w = 0.0227$.

Curves showing the frequency dependence of the modulus of the complex viscosity of the solutions are plotted in Fig. 4. By normalising the values of $|\eta^*|$, the resulting curves superpose rather well giving a unique curve, independent of the concentration (see Fig. 5) if the results are plotted against the reduced frequency $\omega_r = \omega\langle \tau \rangle$. By assuming that Eq. (3) holds, the master curve also would give the variation of the normalised viscosity with the shear rate in a steady flow experiment. The curve representing the variation of the viscosity with the reduced frequency presents a plateau, in which the viscosity hardly varies with the shear rate, followed by another zone (non-Newtonian region) in which the viscosity strongly decreases as the shear rate increases.

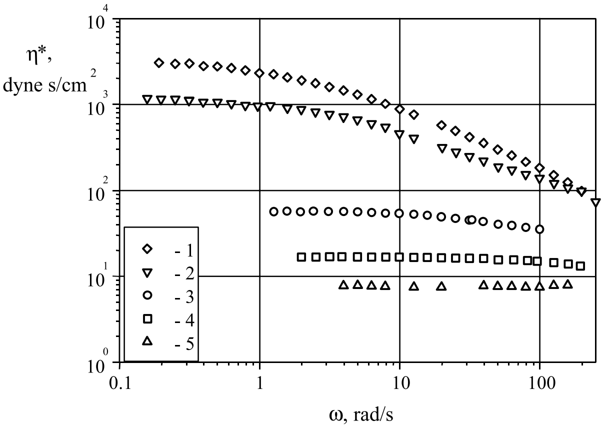

Fig. 4. Absolute values of the complex viscosity, in the frequency domain, for different concentrations: (1) $w = 0.174$, (2) $w = 0.135$, (3) $w = 0.0818$, (4) $w = 0.0533$ and (5) $w = 0.0227$.

Table 1
Characteristic rheological parameters of the solutions

Weight fraction of polymer, w	η_0(dyn s cm^{-2}, steady test)	η_0(dyn s cm^{-2}, oscillatory test)	$10^4 \times J_e^0$ (cm^2 dyn^{-1})	$10^3 \times \langle\tau\rangle$ (s)	$\dot{\gamma}_c$ (s^{-1})
0	7.64 ± 0.07				
0.0227	8.2 ± 0.4	7.8 ± 0.6	1.5 ± 0.7	1.23	813
0.0533	18 ± 1	16.6 ± 0.6	2.6 ± 0.2	4.68	210
0.0818	60 ± 3	58 ± 3	2 ± 1	12	83
0.135	1200 ± 100	1100 ± 300	2.3 ± 0.3	276	3.6
0.174	3700 ± 300	3300 ± 300	2.9 ± 0.9	1070	0.93

3.2. Flow behaviour from steady experiments

With the aim of investigating the reliability of the dependence of the viscosity on the shear rate predicted by the Cox–Merz approach, steady flow experiments were conducted on the solutions, from which the variation of the viscosity with the shear rate was obtained. The pertinent results are shown in Fig. 6. All the curves exhibit a plateau whose length increases as the concentration decreases. The values of the zero-shear rate viscosity obtained for the solutions from steady experiments are shown in the second column of Table 1. It can be seen that these values are in rather good agreement with those obtained from oscillatory experiments by means of Eq. (1). The two solutions with $w = 0.174$ and $w = 0.135$ display shear-thickening behaviour for $\dot{\gamma} > 1\ \mathrm{s}^{-1}$ and $\dot{\gamma} > 4\ \mathrm{s}^{-1}$, respectively, but the solutions with $w \leq 0.0085$ apparently exhibit shear-thinning behaviour at higher shear rates.

Semidilute and dilute polymer solutions are entangled systems, and the density of entanglements increases as the molecular weight and the concentration increases. Below a certain critical concentration, molecular chains do not overlap their domains, and whenever the flow remains in the laminar regime, the solutions exhibit Newtonian behaviour at any shear rate. As long as $\langle\tau\rangle$ is larger than the reciprocal of the shear rate, the systems display Newtonian behaviour. Therefore, it seems that a critical shear rate, $\dot{\gamma}_c$, exists above which the flow behaviour of polymers is no longer Newtonian. The value of this quantity can roughly be estimated by means of the approximation [10]

$$\eta_0 J_e^0 \dot{\gamma}_c \cong 1. \tag{6}$$

Values of the mean-relaxation time and the critical shear rate for the solutions are shown, respectively, in the fifth and sixth columns of Table 1. An inspection of the curves shown in Fig. 6 indicates that departure of the two more concentrated solutions ($w = 0.174$ and 0.135) from Newtonian behaviour occurs at shear rates of roughly 1 and 4 s^{-1}, respectively, in agreement with the predictions of Eq. (6), 0.93 and 3.6 s^{-1}, respectively. The predictions concerning the critical shear rate of the other solutions that display shear-thinning behaviour seem to be in fair agreement with the experimental results.

The curves depicting the dependence of the viscosity on the shear rate obtained from steady flow experiments and from dynamic experiments are rather similar in the case of the shear-thinning solutions. However, the Cox–Merz approximation is not suitable to describe the steady flow behaviour of shear-thickening solutions.

The time necessary to obtain steady-state conditions in the flow of the shear-thickening solutions was investigated by recording the transitory appearing after sudden application

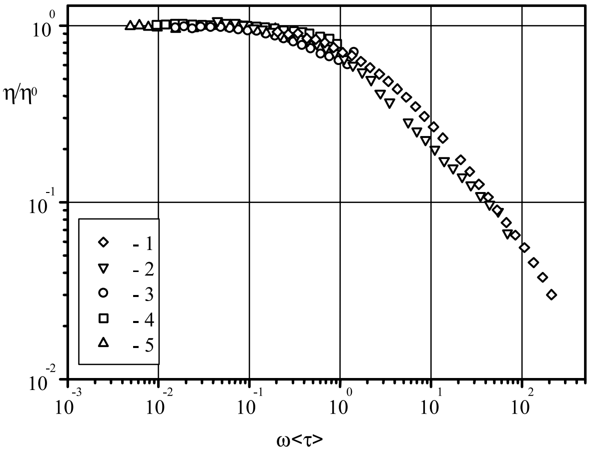

Fig. 5. Master curve for the reduced modulus of the complex viscosity plotted against the reduced frequency: (1) $w = 0.174$, (2) $w = 0.135$, (3) $w = 0.0818$, (4) $w = 0.0533$ and (5) $w = 0.0227$.

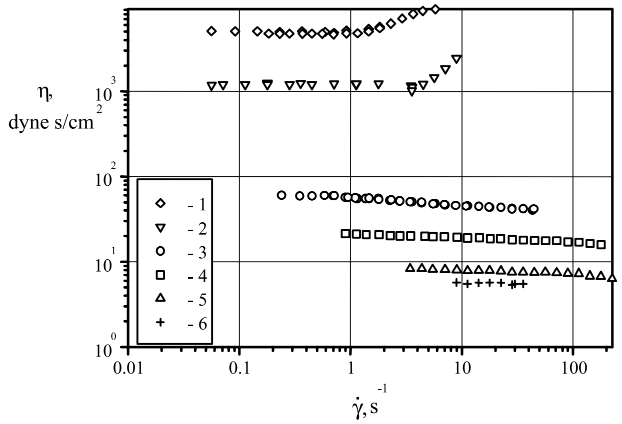

Fig. 6. Shear-rate dependence of the steady-shear viscosity for different concentrations: (1) $w = 0.174$, (2) $w = 0.135$, (3) $w = 0.0818$, (4) $w = 0.0533$, (5) $w = 0.0227$ and (6) glycerine.

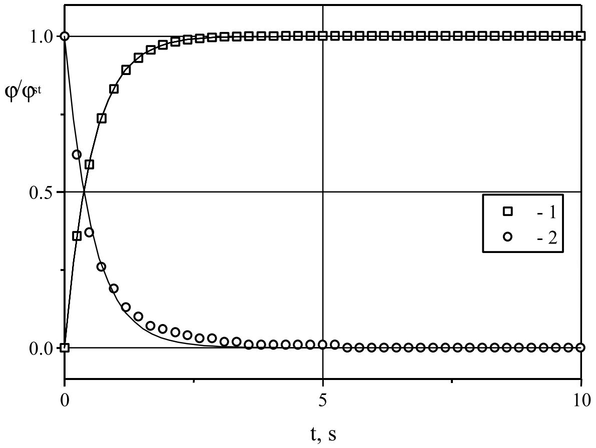

Fig. 7. Transitories after application (1) a shear rate of $1.10\ \mathrm{s}^{-1}$ to the $w = 0.135$ solution and then suddenly cancelling the shear rate (2) after steady flow conditions are reached; $\varphi/\varphi_{\mathrm{st}}$ is the normalised angular displacement, where φ_{st} is the steady displacement. The solid lines are fitting results by the single exponential Eq. (7). For the two transitories, $\tau = 1.84$ s. In both cases, the mean square errors of approximation are less than 0.02%.

of a given shear rate to a well-rested solution. The transient appearing after the sudden cancellation of the steady flow $(\dot{\gamma} = 0)$ was also recorded. These transients for the solution $w = 0.135$, at the shear rate $1.10\ \mathrm{s}^{-1}$ $(<\dot{\gamma}_c)$, are shown in Fig. 7. It can be seen that after the application of the shear rate indicated, steady-state conditions are reached in less than 2 s. The transients expressed in terms of the angular displacement, φ_{st}, are characterised by single exponent functions

$$\varphi = \varphi_{\mathrm{st}}(1 - \exp(-t/\tau)) \quad \text{and} \quad \varphi = \varphi_{\mathrm{st}} \exp(-t/\tau), \tag{7}$$

where the value of the relaxation time, τ, is common for the two expressions.

In the shear-thickening region, the transients are defined by two exponent expressions (see Fig. 8)

$$\begin{aligned} &\varphi(t) = \varphi_{\mathrm{st}}(1 - \exp(-t/\tau_1) - \exp(-t/\tau_2)) \quad \text{and} \\ &\varphi(t) = \varphi_{\mathrm{st}}(\exp(-t/\tau_1 + \exp(-t/\tau_2)) \end{aligned} \tag{8}$$

This behaviour suggests that in the formation of a structure compatible with $\dot{\gamma}$ in the shear-thickening area, two interacting mechanisms of relaxation times τ_1 and τ_2 intervene. The variation of the smaller relaxation time, τ_1, with the shear rate is presented in Fig. 9, where, for comparative purposes, the shear-rate dependence of the normalised viscosity is also shown. It can be seen that τ_1, like the viscosity, remains nearly constant until a critical shear rate is reached after which τ_1 decreases whereas the viscosity increases. The evolution of τ_2 is not so definite. Thus, in the shear-thickening region, the value of τ_2 increases with the shear rate and then decreases.

The variation of the viscosity of well-rested semidilute solutions with time, following the application of a finite shear rate greater than $\dot{\gamma}_c$, is illustrated in Fig. 10. Although

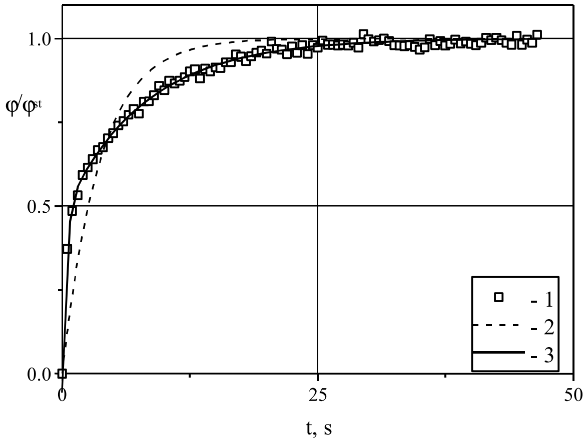

Fig. 8. Transitory, expressed in terms of the normalised angular displacement, $\varphi/\varphi_{\mathrm{st}}$, after the sudden application of a shear rate of $7.12\ \mathrm{s}^{-1}$ to the $w = 0.135$ solution. The dashed line (2) corresponds to the fitting by a single exponent $\varphi/\varphi_{\mathrm{st}} = 1 - \exp(-t/3.67)$ with the error 0.4%. The solid line is the result of two exponents fitting $\varphi/\varphi_{\mathrm{st}} = 1 - 0.52\exp(-t/7.96) - 0.53\exp(-t/0.39)$ with error 0.01%.

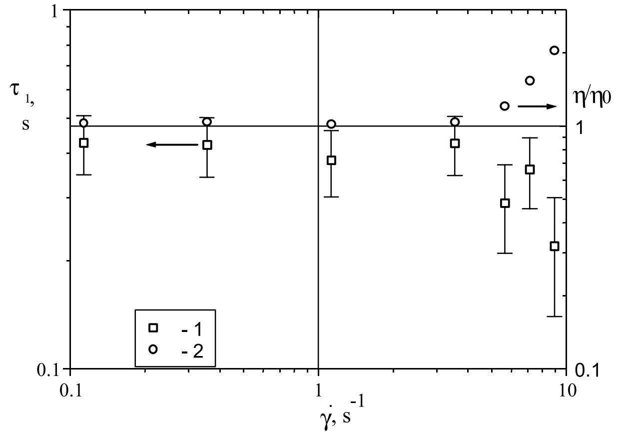

Fig. 9. Dependence of the exponent τ_1 on γ after application of shear stresses to a well-rested $w = 0.135$ solution. The variation of the viscosity with the shear rate is also shown.

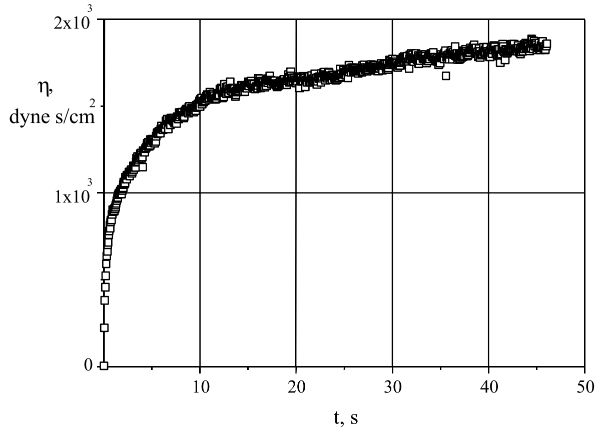

Fig. 10. Evolution of the viscosity with time for the $w = 0.135$ solution after application of the shear rate $7.12\ \mathrm{s}^{-1}$.

the viscosity of the system sharply increases at short times, reaching a steady plateau may take 25 or more seconds. It is important to note that the shape of the curve could depend on the flow geometry [11]. A universal feature of most shear-thickening systems is the relatively large fluctuations undergone by the viscosity in the vicinity of the critical shear rate. These fluctuations, which are rather large in low-concentration micellar solutions, are relatively small in the solutions used in this study [12].

A still unsolved issue in fluid dynamics is the elucidation of the origin of shear-thickening behaviour. The literature shows that this behaviour is not restricted to any particle size range and has been reported for systems having particle sizes below 1 μ up to 500–700 μ as well as for some polymer solutions [13]. Very low concentration solutions of wormlike micelles also exhibit a marked shear-thickening behaviour [14]. In the last years, a great deal of theoretical work has been developed related with shear-induced phase transitions and mechanical instability in complex fluids [15,16]. Careful experiments carried out on solutions of wormlike micelles in which rheological and visualisation techniques have been combined, indicate that these systems exhibit inhomogeneous flow and structure formation. However, it is not possible to conclude whether the changes observed should be regarded as a kind of shear-induced phase transition or merely as a mechanical instability.

Hydrogen bonding between carbonyl and amide groups (–NH···O=C–) stabilises the α helix in poly(α-amino acids) and proteins [17]. Solutions of poly(γ-benzil-L-glutamate) in cresol exhibit a usual high viscosity caused by the existence of small helices along the chains stabilised by –NH···O=C– bonds [18]. In dichloroactic acid solutions, the helices are destroyed, and the viscosity undergoes a sharp decrease. In this later solvent, poly(γ-benzil-L-glutamate) behaves as a flexible coil [18]. In the case of the semidilute solutions studied in this work, shear rates above a critical value presumably promote the development of molecular structures through –NH···O=C– bonds that enhance the viscosity of the solutions. As a result, correlation between dynamic and steady flows only can be established for polymer systems, whose chemical structures do not favour the formation of molecular associations. It is worth noting that the flow behaviour of the solutions described in this work differ from that exhibited by dilute solutions of high molecular weight fractions of polyoxyethylene in mixtures of glycerine:water (50:50) [19]. In spite of the fact that hydrogen bonding between the solvent and the polymer may exist in these systems, high shear rate fields do not promote the formation of molecular associations that enhance the viscosity of the polyoxyethylene solutions. Therefore, these solutions only present shear-thinning behaviour and, as a result, the Cox–Merz approximation fits rather well the results obtained from direct steady experiments.

In general, macromolecular fluids of flexible backbone can be crudely viewed as a mass of entangled chains, therefore having a 'structure'. The entanglement degree (e.g. the number of entanglements/chain) in polymer solutions depends on molecular weight and concentration. The crossover between dilute solutions, where the coils are separated, and more concentrated solutions, where the coils overlap, is expected to occur at a concentration, c^*, comparable with the concentration inside a single chain of N segments so that, for a good solvent, $c^* \sim a^3 N^{-4/5}$, where a^3 is the volume of a segment of the chain [20]. In terms of the polymer fraction, the threshold $w^* \sim N^{-4/5}$ will occur at roughly 10^{-2} in the solutions used in this work. In view of this and due to the relatively low molecular weight of the poly(2-hydroxyethyl methacrylamide), one would expect that the chains in these solutions, even the higher concentrated ones, would be loosely entangled. Therefore, the structure that evidently displays the solutions must arise, as indicated above, from hydrogen bonding between the carbonyl and the amide groups. As the concentration increases, overlapping between the molecular domains also augments, and as a result, the looseness of the structure decreases. The structure of the solutions is dynamic, and it is characterised by the mean-relaxation times indicated in the fifth column of Table 1. One would expect a linear relationship between shear stress and shear rate (constant viscosity) for the solutions, whose structure is not changing during laminar flow conditions. This occurs when the experimental time window, expressed in terms of the reciprocal of the shear rate, is larger than the mean-relaxation time of the structure of the solutions. The flow behaviour of the solutions for shear rates at which $(1/\dot{\gamma}^{-1}) < \langle \tau \rangle$ depends on concentration. For semidilute solutions ($w = 0.135$ and 0174), the experimental results suggest that shear rates above a critical value promote the formation of more tight structures. In this case, the response time of the molecules of the structure is too large relative to the experimental time window and, as a result, the viscosity increases with the shear rate. The opposite seems to occur in the shear-thinning solutions.

4. Conclusions

The dilute and semidilute solutions of poly(2-hydroxyethyl methacrylamide) in glycerine display linear viscoelastic behaviour at very low shear rates. The steady-state compliance function J_e^0 is independent of the concentration of polymer in the solution, but the zero shear rate viscosity, η_0, is strongly dependent on concentration.

Semidilute and dilute solutions exhibit, respectively, shear-thickening and shear-thinning behaviour. The non-Newtonian behaviour of the semidilute solutions cannot be obtained from dynamic (oscillatory) measurements.

To reach steady flow conditions in the non-Newtonian region, the semidilute solutions need a relatively long time. Therefore, these solutions exhibit rheopectic behaviour in the non-Newtonian zone.

Formation of tight structures in semidilute solutions through hydrogen bonding between acrylamide and carbonyl groups of different chains, at relatively high shear rate, is presumably responsible for the shear-thickening behaviour of the semidilute solutions.

Acknowledgements

This work was supported by the DGICYT through the Grant 96-0134-C02-01. One of us (S.R. Kosvintsev) is indebted to the DGICYT (Estancias Temporales de Científicos Extranjeros en España) for a fellowship.

References

[1] Vinogradov GV, Malkin AYa. Rheology of polymers. New York: Springer, 1980.

[2] Ferry JD. Viscoelasticity of polymers. 3rd ed. New York: Wiley-Interscience, 1980.

[3] Covas JA, Agassant JF, Diogo AC, Vlachopoulos J, Walters K, editors. Rheological fundamentals of polymers processing. NATO ASI Series. 1994.

[4] Carreau PJ, De Kee DCR, Chhabra RP. Rheology of polymeric systems. Munich: Hanser Publishers, 1997.

[5] Riande E, Díaz-Calleja R, Prolongo M, Masegosa R, Salom C. Polymer viscoelasticity: stress and strain in practice. New York: Marcel Dekker, 2000.

[6] Vinogradov GV, Malkin AYa. Rheology of polymers. New York: Springer, 1980. p. 294.

[7] Vinogradov GV, Malkin AYa. Rheology of polymers. New York: Springer, 1980. p. 284.

[8] Cox W, Merz E. J Polym Sci 1958;28:619.

[9] Riande E, Díaz-Calleja R, Prolongo M, Masegosa R, Salom C. Polymer viscoelasticity: stress and strain in practice. New York: Marcel Dekker, 2000. p. 252 (also see p. 368).

[10] Graessley WW. Viscoelasticity and flow in polymer melts and concentrated solutions. In: Mark JE, editor. Physical properties of polymers. Washington: ACS, 1984. (Chapter 3).

[11] Hu YT, Matthys EF. Rheol Acta 1995;34:450.

[12] Hu YT, Boltenhagen P, Pine. J Rheol 1998;42:1185.

[13] Bauer WH, Collins EA. In: Eirich FR, editor. Thixotropy and dilatancy, 4. 1967. p. 454 (Chapter 8 and references therein).

[14] Hu YT, Boltenhagen P, Matthys E, Pine. J Rheol 1998;42:1209.

[15] Cates ME, McLeish TCB, Marrucci G. Europhys Lett 1993;21:451.

[16] Porte G, Berret J-F, Harden JL. J Phys II 1997;7:459.

[17] Tanford C. Physical chemistry of macromolecules. New York: Wiley, 1961. p. 50.

[18] Yang JT. J Am Chem Soc 1958;80:1783.

[19] Ortiz ME, De Kee D, Carreau. J Rheol 1994;38:519.

[20] De Gennes PG. Scaling concepts in polymer physics, 2nd ed. Ithaca: Cornell University Press, 1985. p. 76.